Absolute surface free energies of perfect low-index orientations of metals and semiconductors

H. P. Bonzel*
Institut für Schichten und Grenzflächen, ISG 3, Forschungszentrum Jülich GmbH, D-52425 Jülich, Germany

M. Nowicki
Institute of Experimental Physics, University of Wrocław, Pl. Maxa Borna 9, 50-204 Wrocław, Poland
(Received 11 June 2004; published 27 December 2004)

Absolute experimental surface free energies of low-index metal and semiconductor surfaces are practically nonexistant. To obtain these fundamentally important parameters, quantitative measurements of absolute step free energies and equilibrium shapes of three-dimensional crystallites for a particular material and facet orientation are needed. The current work is an evaluation of some absolute surface free energies, based on the above concept, for well-defined Au(100), Cu(111), Cu(100), Pb(111), Si(111), and Si(100)-2×1 surface orientations. A comparison with previous experimental and theoretical surface free energies shows good agreement for Au and Pb but substantial discrepancies and scatter for Cu and Si. Possible reasons for this surprising result are pointed out.

DOI: 10.1103/PhysRevB.70.245430 PACS number(s): 68.35.Md, 68.35.Bs, 68.55.Jk

I. INTRODUCTION

Surface free energies of crystalline metals and semiconductors are notoriously difficult to measure and experimental values of this fundamentally important parameter for well-defined low-index orientations are practically unknown.[1–3] The only source of information are theoretical values obtained by more or less rigorous approaches.[4–13] The spread in theoretical values is substantial, as pointed out, for example, for Pb surfaces.[14] The lacking comparison of theoretical and experimental low-index surface free energies constitutes a highly unsatisfactory situation. A principal remedy for this dilemma may result from a detailed study of three-dimensional (3D) crystallites in their thermodynamic equilibrium shape (ECS). Crystallites which exhibit continuous facet-to-vicinal transitions are in principle an image of free energy relationships according to Wulff's theorem.[15–17] In particular, the radius of a facet (in a high symmetry direction), divided by the distance between that facet and the center of the 3D crystallite, is proportional to the ratio of step over surface free energy.[18] This relation is illustrated in Fig. 1 which shows a cross section of a 3D crystallite. The outline is $z(x)$, with a principal facet of radius r_f located at $z=z_0$. The transition between the facet and the vicinal range is continuous. The mentioned relationship is as follows:[18,19]

$$\frac{r_f(T)}{z_0(T)} = \frac{f_1(T)}{f_0(T)}, \tag{1}$$

with $f_0(T)$ as the surface free energy of the (stepless) facet and $f_1(T)$ as the free energy of the step bounding the facet. Whenever either $f_0(T)$ or $f_1(T)$ is known, the other can be calculated using the experimentally measurable ratio $r_f(T)/z_0(T)$.

For Eq. (1) to be valid, full thermodynamic equilibrium of the 3D crystallite has to be assured. This requires sufficiently long annealing times at a temperature T where diffusion kinetics is fast enough to enable shape equilibration. Certain precautions have to be taken if equilibration is carried out under vacuum conditions.[20] Crystallite sizes should be in the range of the "thermodynamic limit." They also should exhibit a certain dislocation density to avoid the problem of the large activation barrier for facet growth or shrinkage[21,22] which may hinder the realization of a true equilibrium state for defect-free crystallites. The latter two requirements are usually fullfilled for crystallite radii of the order of μm.[14,23,24] When only a single step is present within the area of a facet, due to a screw dislocation threading the surface, the problem due to the activation barrier for equilibration of the crystallite is largely eliminated.[25]

Utilizing Eq. (1) in a suitable experiment seems to be the only way to obtain the surface free energy of an ideal low-index orientation, provided the absolute step free energy is available. Any other experiment, such as cleavage of a crystal[1] or a liquid/solid wetting experiment carried out in a temperature gradient,[26] in general will not result in values characteristic of ideal facet orientations. The more common zero creep experiments used to determine surface free energies of metals[27–29] are all carried out for polycrystalline materials yielding a surface free energy averaged over a range of largely unknown orientations.

The measurement of absolute surface free energies, based on quantitative images of 3D crystallite shapes under equilibrium conditions, is possible because of the very substantial

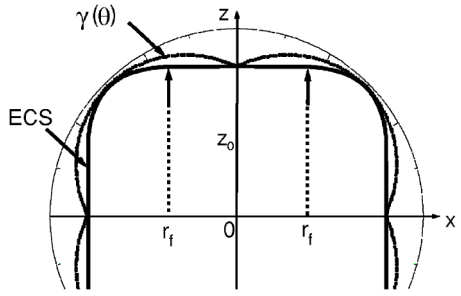

FIG. 1. Schematic cross section of a truncated 3D crystallite on a substrate surface.

progress in determining absolute step and kink formation energies on well-defined crystal surfaces.[30–37] The latter are used to calibrate the energy scale of the 3D ECS. The new objective of utilizing this data for measuring absolute surface free energies of low-index orientations has caused renewed interest in the study of 3D equilibrated crystallites.[2,14,24,38,39] The current work draws attention to this general issue and compares various experiments carried out on two-dimensional (2D) and 3D equilibrium shapes of Si and some metals which allow us to determine the surface free energy of a well-defined low index surface. A brief comparison with theory concludes this survey. The general comparison of the most recent studies suggests that experimental and theoretical values of surface free energies of silicon and several metals may be of questionable accuracy.

II. 2D EQUILIBRIUM CRYSTAL SHAPES AND ABSOLUTE STEP FREE ENERGIES

The current route to absolute surface free energies is via the primary determination of absolute step free energies. Therefore we review briefly the published results for those materials for which we intend to derive an absolute surface free energy of a facet orientation. The key relationships for determining absolute step free energies from equilibrium shapes are the Wulff theorem and the Gibbs-Thomson equation applied to the boundary of 2D islands and facets of 3D crystallites.[2,30,34,36] The following equation couples the product of the step radius, r_{fi}, of a 2D island times the local (minimum or maximum, depending on step) step curvature, K_i, to the most important thermodynamic step properties, the step free energy, $f_1(T)$, and the step stiffness, $\tilde{f}_1(T)$:

$$r_{fi}(T)K_i(T) = \frac{f_{1i}(T)}{\tilde{f}_{1i}(T)}, \tag{2}$$

for step i. This relationship has been recognized to be one of the keys for the determination of step and kink formation energies from 2D ECS. According to Eq. (2), experimental $r_f(T)K(T)$ data for a particular equilibrium shape step are fit to theoretical expressions of $f_1(T)/\tilde{f}_1(T)$.[34,36,37,39] We return to this further below.

Historically, absolute step free energies at a single temperature have been derived from step fluctuations on Si(100) surfaces.[40] Because of the reconstruction of this surface there are inequivalent *A* and *B* steps. At 900 K, for example, the *A* step remains nearly straight due to a high kink formation energy, whereas the *B* step meanders with a large amplitude. Kinks on one step are made up by steps of the other type. Hence a low (high) step energy correlates to a high (low) kink energy. In addition there is a kink corner energy of considerable magnitude in this case.[40] A related study by Zandvliet *et al.*[41] utilizing "freeze-in temperatures" of step fluctuations led to similar values of single height step free energies of Si(100). A different approach was used by Bartelt *et al.*[30] who evaluated 2D island equilibrium shapes on Si(100) at different temperatures. Assuming elliptical island shapes, they determined step radii and local step curvatures of *A* and *B* steps and from those the corresponding step free energies. These experiments dealing with Si(100) and Si(111) energetics are reviewed in Refs. 32 and 33.

Extensive work on metal surfaces has demonstrated that absolute step free energies can be reliably measured from equilibrated 2D crystallites (adatom or vacancy islands of monolayer thickness). Several approaches have been proposed and tested. In the first approach, the magnitude of spatial fluctuations of the bounding island step is determined quantitatively as a function of the island's mean radius, r_f, and temperature.[42,43] It is shown that the time and azimuth averaged fluctuation amplitude is proportional to $r_f T$ divided by the mean step free energy. This technique has been applied to Cu(111), Cu(100), and Ag(111) surfaces. In a second approach the temperature variation of the equilibrium island shape is the source for a quantitative evaluation of step free energies.[34,44] The imaged island shapes were evaluated in different ways, utilizing either temperature-dependent aspect ratios or products of step radii times step curvature, according to Eq. (2).[34] A comparison of both the step fluctuation and equilibrium island shape techniques applied to the same metal surfaces yielded consistent results.[43] Quantitative expressions for the temperature dependence of step free energies and stiffnesses derived in the framework of Ising theory play an important role in most of these evaluations. More recently it has been shown that including next-nearest-neighbor interactions into the evaluation of Cu(100) improves the agreement between experiment and theory.[45]

A third approach for obtaining absolute step free energies was proposed in connection with studying 3D crystallite shapes at various temperatures.[2,46] Here the temperature-dependent radius of a facet on a fully equilibrated 3D crystallite has to be measured. Since $r_f(T)$ is directly proportional to the step free energy, the data can be fitted by a two- or three-parameter theoretical expression which describes the temperature dependence of the step free energy. The fit would yield the step energy at 0 K, the kink formation energy and a constant vibrational step entropy. First experiments have shown that Ostwald ripening, taking place in an ensemble of crystallites on the support surface, is seriously interfering with the observation of a single crystallite whose facet is the prime object of investigation.[46] Any volume change of that crystallite caused by Ostwald ripening will falsify the change in facet radius which is expected to correlate with a change in temperature only, independent of any time effects. Hence no useful results have been obtained with this approach.

To proceed in the sense of Eq. (2), we discuss briefly the temperature dependence of the step free energy and step stiffness. In general, surface steps in a high symmetry direction are perfectly straight at 0 K and develop increasing roughness at elevated temperatures because an increasing density of kinks is produced by thermal excitation. Hence the step free energy decreases with increasing temperature. The step stiffness, on the other hand, being a measure of the resistance to step meandering, is infinite at 0 K and decreases steeply with increasing temperature. To a first order, i.e., for $\varepsilon_k \gg kT$, these quantities are described by the following equations (for a hexagonal lattice):

$$f_1(T) = 2\varepsilon_k - 2kT\exp\left(-\frac{\varepsilon_k}{kT}\right), \tag{3}$$

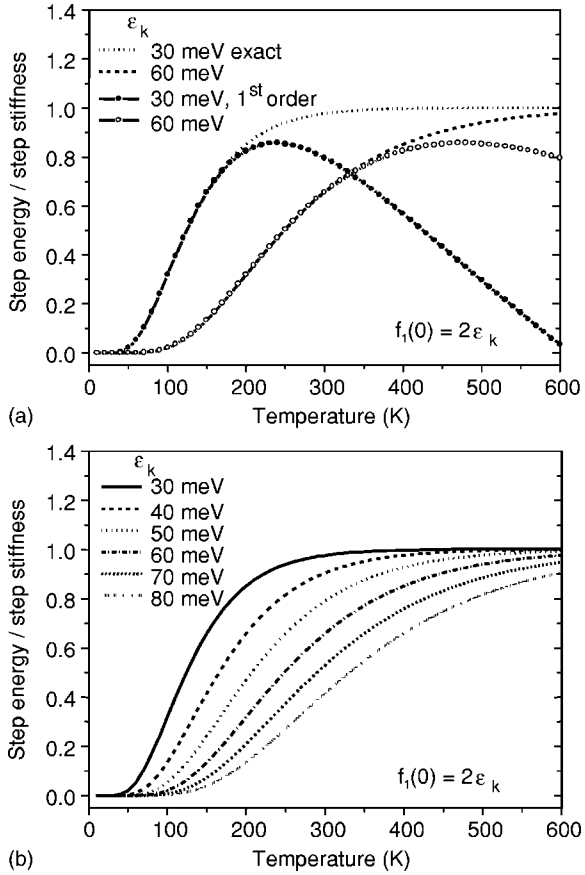

FIG. 2. (a) Plot of first order and exact $f_1(T)/\tilde{f}_1(T)$ ratio functions versus temperature for two selected values of kink energies. (b) Plot of exact $f_1(T)/\tilde{f}_1(T)$ ratio function versus T for a range of kink energies, according to the Akutsu theory (Ref. 47).

$$\tilde{f}_1(T) = \frac{2kT}{3}\exp\left(\frac{\varepsilon_k}{kT}\right). \tag{4}$$

Similar expressions hold for square lattices.[34] Taking the ratio $f_1(T)/\tilde{f}_1(T)$, one obtains a function which increases from zero at low temperature to a maximum of less than 1 at T near $(2/3)\varepsilon_k/k$, such as illustrated in Fig. 2(a) for two kink energies. The fact that $f_1(T)/\tilde{f}_1(T)$ does not reach 1 and even decreases beyond the maximum is a consequence of the approximate nature of Eqs. (3) and (4). A circular island, defined by $f_1(T)/\tilde{f}_1(T)=1$, is expected at high temperatures,[18] and once this has been reached, it should remain circular. Indeed, corresponding second order[36] and especially the exact expressions[47] for $f_1(T)/\tilde{f}_1(T)$ show the expected asymptotic behavior towards 1 at high temperature, regardless of the value of the kink energy. This is also illustrated in Fig. 2(a). Consequently, if island shape changes are followed over a large range of temperatures, it is necessary to use the exact expressions for $f_1(T)/\tilde{f}_1(T)$. The higher the kink energy, the higher the temperature where $f_1(T)/\tilde{f}_1(T)$ begins to rise. A plot of the exact ratio versus temperature for a series of kink energies between 30 and 80 meV is shown in Fig. 2(b).[39] The step energy at 0 K for a hexagonal Ising lattice is equal to $2\varepsilon_k$.

Next we briefly discuss the problem associated with anisotropic 2D islands. The Ising model considers nearest-neighbor interactions only. It is therefore not surprising that the Ising formalism developed for a thermodynamic description of steps is well suited for close-packed steps where nearest-neighbor interactions are more important than next-nearest-neighbor interactions. This point seems to be important when the step energy of a 2D island is anisotropic which is the case when two kinds of structurally inequivalent steps are bounding the island, such as for (111), (100), and (110) surfaces of fcc metals or for the reconstructed Si(001)-2 $\times 1$ and the nonreconstructed Si(111)-1$\times$1 surfaces, for example. Each step has then a specific step and kink formation energy. The step with the lower free energy (for metals called the *B* step) has a higher kink energy than the other step of higher free energy (called the *A* step). Hence the *A* step becomes round at lower temperature. It is obvious that a strict relation between step and kink energy, $f_{1i}(0)=c\varepsilon_{ki}$ (with c =const), cannot hold for both types of steps. Recent measurements for Pb(111) demonstrated this very clearly by step energies of 116 and 128 meV, and kink energies of 60.6 and 42.5 meV, for *B* and *A* steps, respectively. The Ising condition $f_1(0)=2\varepsilon_k$ is closely obeyed for the *B* step but not at all for the *A* step which has a more open structure. A similar situation is encountered for Cu(100) where the close-packed $\langle 110\rangle$ step has a step energy of 220 meV and a kink energy of 128–131 meV.[35,48] By taking nearest- and next-nearest-neighbor interactions into account and fitting the experimental shape anisotropy data, separate formation energies of the close-packed $\langle 110\rangle$ step and the open $\langle 010\rangle$ step of 193 and 227 meV, respectively, were determined.[45] These correspond to an island anisotropy of 1.18 at 0 K, compared to 1.24 experimentally and 1.41 if both steps were Ising-like. Also for Si(001)-2×1 which is a surface of two fold symmetry, the inequivalent steps have very different energies of 140 and 56 meV, respectively.[33]

The reason for going into so much detail here is that the different types of steps of anisotropic islands cannot both be evaluated with the Ising model equations involving step curvatures, such as in Eq. (2). The curvatures of the step with higher step free energy depend on the presence of the more stable step of lower free energy. Hence the products $r_i(T)K_i(T)$ derived for the high energy step can become larger than 1 which in fact was observed for Pb(111).[36,37] In other words, the local curvature $K_i(T)$ is then larger than $1/r_{fi}(T)$. This effect never occurs for the lower free energy step. The study of 2D equilibrium shape islands on Si(001) also shows this very clearly.[30] The elliptic island shape allows a simple calculation of the minimum (maximum) step curvature for *A* and *B* steps, according to $K_A(T)=r_{fA}/r_{fB}^2$ and $K_B(T)=r_{fB}/r_{fA}^2$, respectively. Hence the product $r_{fA}(T)K_A(T)$ is simply $(r_{fA}/r_{fB})^2$ which is also equal to $1/[r_{fB}(T)K_B(T)]$. Since the anisotropy $r_{fA}/r_{fB}<1$, $r_{fA}(T)K_A(T)$ increases with temperature to asymptotically approach 1 whereas $r_{fB}(T)K_B(T)$ is always larger than 1 and decreases with temperature towards 1. Step free energies are in this case very different, in the range of 52–60 and 120–180 meV for *A* and

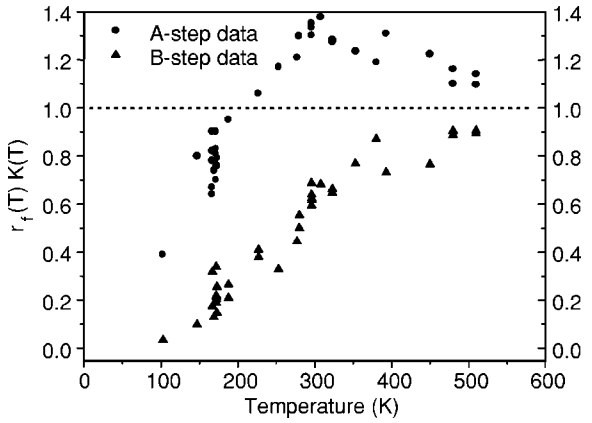

FIG. 3. Plot of experimentally measured $r_{fA}(T)K_A(T)$ and $r_{fB}(T)K_B(T)$ versus temperature for *A* and *B* steps of vicinal Pb(111) surfaces. The data result from STM images of 2D island and (111) facet shapes (Ref. 37).

B steps, respectively,[33,40,41,49] with kink energies of 180 and 56 meV.[33,40]

The general behavior outlined above has been observed for 2D islands of Pb(111).[36,37] Islands as well as (111) facets on 3D ECS of Pb are three fold symmetric, with *B* steps having the lower free energy. Combining experimental data obtained from analyzing facet shapes and 2D island shapes over a large range of temperature, $r_i(T)K_i(T)$ data were evaluated for both types of steps, such as seen in Fig. 3. The data for the low-energy *B* step are less than 1 and approach 1 at high temperature whereas the *A*-step data are less than 1 only at low temperature, rise above 1, and then decrease towards 1 at high temperature. The *B*-step data were fit with the exact Akutsu equations[47] for $f_1(T)/\tilde{f}_1(T)$, resulting in reliable energy data for *B* steps quoted above. The quality of the fit and the fact that $f_{1B}(T)$ is close to $2\varepsilon_{kB}$ justify this Ising model approach. The same experimental data would also permit a one-parameter fit with just the kink energy, resulting in $\varepsilon_{kB}=62$ meV and $f_{1B}(T)=124$ meV. The *A*-step data for the same islands, on the other hand, were evaluated by fitting the island anisotropy versus temperature, keeping the step and kink energy of *B*-steps fixed. This resulted in the energetic data of *A* steps where $f_{1A}(T)$ is about equal to $3\varepsilon_{kA}$, a ratio in conflict with the Ising condition. The *A*-step data are consistent with the *B*-step data in the framework of a simple awning approximation[50] which relates the ratio of kink energies to the island anisotropy ratio at 0 K:

$$\frac{\varepsilon_{kA}}{\varepsilon_{kB}}=\frac{1-0.5f_{1A}/f_{1B}}{f_{1A}/f_{1B}-0.5}. \tag{5}$$

Taking the extrapolated anisotropy ratio of 1.104 at 0 K and $\varepsilon_{kB}=62$ meV, one obtains $\varepsilon_{kA}=46$ meV and $f_{1A}(T)=137$ meV. These values are in good agreement with the data evaluated from the temperature-dependent island anisotropy.[23,37] The experimental results on step energies quoted here are furthermore supported by recent density functional theory of step energies of Pb(111).[51]

III. ABSOLUTE SURFACE FREE ENERGIES: RESULTS AND DISCUSSION OF RECENT EXPERIMENTS

Together with the Wulff theorem of Eq. (1) and a quantitative image of the 3D ECS at a particular temperature *T*, the absolute step free energies at *T* are the entry to absolute surface free energies of facet orientations. Hence it is clear that at least two independent experimental results are needed to determine the surface free energy of a facet orientation, namely the geometric ratio $r_f(T)/z_0(T)$ from a 3D regular ECS (with no orientations missing) and the free energy $f_1(T)$ of the step which is the boundary of that particular facet. For anisotropic surfaces possibly two different step free energies and $r_f(T)/z_0(T)$ ratios may be involved. Some authors prefer three separate measurements to be more independent of theoretical model expressions describing the temperature dependence of $f_1(T)$ or the ratio $f_1(T)/\tilde{f}_1(T)$.[38]. The relevant expression is then[38]

$$f_0(T)=\frac{f_1(T)}{\tilde{f}_1(T)}\tilde{f}_1(T)\frac{z_0(T)}{r_f(T)}. \tag{6}$$

The ratio $f_1(T)/\tilde{f}_1(T)$ is measured from the 2D ECS through the use of Eq. (2), the stiffness $\tilde{f}_1(T)$ is independently obtained from a statistical evaluation of single step fluctuations at *T*, and finally $z_0(T)/r_f(T)$ is measured from the 3D ECS at the same temperature. In this case the uncertainties of three measurements enter into calculating the surface free energy at a particular *T*.

The evaluation of the 3D ECS is more involved when the transition between facet and vicinal surface is discontinuous, i.e., characterized by a finite slope p_f. In general, the ratio $f_1(T)/f_0(T)$ will be larger than $r_f(T)/z_0(T)$.[52] When the discontinuity is due to mixed repulsive and attractive step interactions ($f_3<0, f_4>0$), the relationship (1) was shown to change to[53]

$$\frac{r_f(T)}{z_0(T)}(p_f>0)=\frac{f_1(T)}{f_0(T)}+\frac{4f_3(T)}{27f_0(T)}\left(\frac{f_3}{f_4}\right)^2, \tag{7}$$

$$p_f=-\frac{2f_3}{3f_4}. \tag{8}$$

However, an evaluation according to Eq. (7) is considerably more complicated because the quantities $f_3(T)$ and $f_3(T)/f_4(T)$ have to be determined in addition to $r_f(T)/z_0(T)$. This requires a detailed evaluation of the round portion of the ECS adjacent to the facet, as it has been carried out for the ECS of Au crystallites.[53,54] On the other hand, the discontinuity at the facet edge facilitates the experimental determination of r_f by imaging techniques of lower than atomic resolution.

At this point we add some comments regarding experimental requirements. To obtain reliable experimental values of $z_0(T)$ and $r_f(T)$ of the 3D ECS at elevated temperature requires high resolution imaging, preferably step-resolved imaging, such as with scanning tunneling (STM) and atomic force microscopies (AFM).[39,55] The same demand holds for the investigation of 2D islands and for studying single step

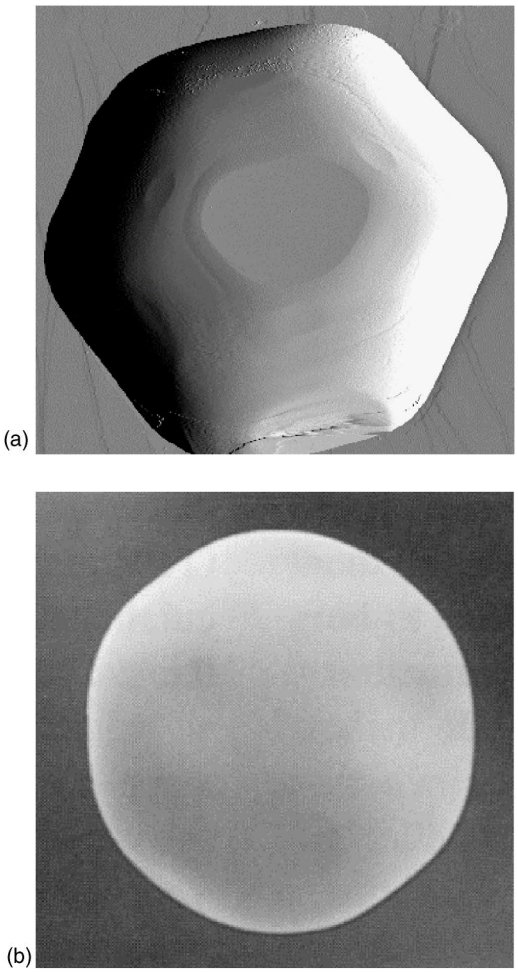

FIG. 4. Experimental images of equilibrated Pb crystallites: (a) STM image of Pb crystallite (diameter: 1.35 μm) with (111) facet and bounding step (Refs. 14 and 39). (b) SEM image of equilibrated Pb crystallite (diameter: 7.5 μm) showing (111) and (100) facets (Ref. 58).

fluctuations on vicinal surfaces. Examples in Fig. 4 show that the boundary of a (111) facet on a Pb crystallite, due to a step of monatomic height, is clearly seen by STM. The STM image shows, furthermore, small {112} and {221} facets which were previously seen only on growth shapes.[56] By comparison, high resolution scanning electron microscopy (SEM) is not capable of resolving facet edges for continuous facet-to-vicinal transitions.[57,58] Interpolation or curve fitting procedures have to be used to estimate facet radii.[59] Reflection electron microscopy (REM) has been used successfully to image single steps and 2D islands at elevated temperature on Si surfaces, especially in context of studying the dynamics of step fluctuations, but severe image distortion limits the accuracy of measuring equilibrium shapes.[60,61] The image of the 3D ECS has to be sufficiently complete such that the Wulff point of the crystallite can be determined. This is essential for measuring the separation of the facet from the Wulff point. Image distortions present in STM images of 3D truncated crystallites can be corrected if several main facets of known orientation are present.[14,39] A linear expansion of the z scale will usually compensate piezorelaxation effects that cause the distortion. The crystallographic angles between different facets on the ECS determine the degree of expansion (or contraction).

Now we proceed to the evaluation of actual experimental data. Only a small number of experiments are available in the literature which allow us to estimate reliable surface free energies from 3D ECS of small crystallites. A survey of these studies and their results are summarized in Table I. The step free energy is calculated for the temperature at which the ECS has been analyzed. Configurational and vibrational entropies were taken into account for metal surfaces but for Si only the configurational entropy was considered.

The best studied solids in this context are Pb and Si. Especially for Si there is an abundance of absolute step free energy and step stiffness data[30,33,40,41,49,66,67] and of 3D ECS studies.[38,60,61,65,68–70] However, only two groups report relative step free energies in the form of $r_f(T)/z_0(T)$ values.[60,65] Note that even at high temperature the step free energy is not necessarily equal to the step stiffness.[38,47] Partial ECSs of Si were obtained for voids of nanometer dimensions[65,69] as well as equilibrated narrow columns of micrometer diameter[60,61] and even cylindrical holes of 0.4 mm diameter.[70] Most groups report stable (111) and (100) facets although the stability of (100) facets under equilibrium conditions has been seriously questioned.[20,70,71] We list in Table I examples of step free energy data, in conjunction with two sets of $r_f(T)/z_0(T)$ values for (111) and (100) surfaces, which have been calculated from derivatives of the anisotropic surface free energy versus orientation, $d\gamma(\Theta)/d\Theta$, at the respective cusps.[60,65] These data were obtained at three different temperatures. A step free energy of 56 meV/Å at 1073 K for the high temperature phase Si(111)-1×1 was reported in early work[72,73] but later much lower values around 14–30 meV/Å seemed more appropriate.[38,60,70,74,75] Because of this uncertainty and the different temperatures involved we prefer to use the results of a model calculation for this surface.[47] The results of this calculation, in which first- and second-nearest-neighbor interactions are taken into account, was matched to quasiexperimental values, originally fit to a surface free energy of 1 J/m^2.[60] The calculated $\tilde{f}_1(T)$ also agrees with the measured step stiffnes of 17 meV/Å at 1373 K.[76]

In most cases we consider high temperature data, i.e., those representing the Si(111)-1×1 and the reconstructed Si(100)-2×1 surfaces. For the twofold symmetric Si(100) we take the average of the A- and B-step free energies which is believed to correlate best with the measured average radius of the (100) facet on the ECS. Here a range of fairly consistent values between 7.6 and 3.5 meV/Å was reported or calculated for the temperatures of the ECS measurement[30,40,41,77] using kink energies of 190 and 120 meV for A and B steps, respectively.[40] Table I shows that the spread in surface free energies calculated for both Si surfaces is large, ranging from 48 to 103 meV/Å^2, corresponding to 0.77–1.64 J/m^2, if we disregard the lowest value of 29 meV/Å^2 for Si(100) at 1323 K. It appears that temperature dependence may be partially responsible for this spread. The values at 973 K fall into a range between 0.77 and 1.64 J/m^2 while those at 1323 K and above are all below 0.85 J/m^2. Despite this possible correlation the overall

TABLE I. Step and surface free energies of well-defined (111) and (100) orientations measured via a quantitative study of 3D crystallites.

Surface	$f_1(T)$ (meV/Å)	T (K)	Reference	$r_f(T)/z_0(T)$	Reference	$\gamma_{111}(T)$ (meV/Å^2)	$\gamma_{111}(T)$ (J/m^2)	Reference
Au(100)	58.9	353	62	0.112 corr	53			Present
	20.7[a]	1123		at 1123 K		90.6	1.46	
				quench				
Cu(111)	102.4	0	43	0.11	64			Present
	57.6	1240		quench		251	4.0	
Cu(100)	83.3	0	43	0.08	64			Present
	49.3	1240		quench		341	5.5	
Pb(111)	28.6–30.7	323	14	0.34–0.35	14	27.5	0.44	14
	27.2–28.7	373		0.33–0.35		average	average	
	26.5–27.9	393		0.31				
Pb(111)	19.3	550	14	~0.25 est.	57	22	0.35	Present
				quench				
Si(111)	35	973	47	0.15	65	75	1.19	Present
Si(111)	20	1323	47	0.12	60	53	0.85	Present
	1×1 phase							
Si(111)	18	1373	47	0.12	38	48	0.77	Present
	1×1 phase							
Si(111)	14.1–19.8	1373	38	0.12–0.14	38, 60, and 61	37–53	0.59–0.8	38
	1×1 phase							
Si(100)	7.6[b]	973	30 and 40	0.054	65	103	1.64	Present
Si(100)	~3.5	973	30 and 40	0.054	65	48	0.77	Present
Si(100)	7.35[b]	973	41	0.054	65	101	1.61	Present
	2.9[b]	1323		(0.076)	60	(29)	(0.47)	

[a]Au step free energy at 1123 K estimated with kink energy of 70 meV[63].

[b]Si(100) average step energy corrected for temperature of ECS measurement with kink energies of 190 and 120 meV for *A* and *B* steps, respectively (Refs. 33 and 40).

result is not very satisfactory for a well studied material such as Si, especially in view of the relatively small surface free energy anisotropy of only 11% at 973 K (Ref. 65) and 3% at 1323 K (Ref. 60) between (111) and (100). Some authors report $\gamma(100)/\gamma(111)>1$ at 873–973 K (Refs. 65 and 69) while another group finds $\gamma(100)/\gamma(111)<1$ at 1323 K.[60,61] This is an unresolved discrepancy which causes further concern. The surface free energies of Si in Table I may be compared with published absolute surface free energies, such as the experimental value of 1.23 J/m^2 for Si(111),[78] and theoretical values (at 0 K) ranging from 1.4 to 1.8 J/m^2.[68,79–83] Here we disregard the relatively small differences due to various forms of reconstruction. It appears that the current values tend to be lower than previously published surface free energies of Si(100) and Si(111). Some of the difference may be due to temperature, an effect whose magnitude is difficult to estimate for such a large range.

For Cu there are excellent absolute step and kink energy data[42,43] which allow the calculation of step free energies at high temperature. The experimental values extrapolated to 0 K agree well with theoretical step energies.[84] However, so far little information on the ECS of Cu crystallites is available.[24,64] Recently, Cu crystallites deposited on sapphire have been equilibrated at 1240 K and quenched to room temperature. *Ex situ* imaging of the crystallites by scanning electron microscopy (SEM) along the ⟨110⟩ direction produced shapes with well developed (111) and (100) facets whose radii were determined by curve fitting with a general shape function.[64] Using the data listed in Table I, calculated surface free energies for both (111) and (100) orientations turn out to be very high, namely 4.0 and 5.5 J/m^2, respectively, compared to published values of the order of 1.85 J/m^2.[1] The large differences calculated for the (111) and (100) orientations are also inconsistent with the experimental low anisotropy of the surface free energy (~2%) at this high temperature.[24]

A special case is Au where the transitions between (111) and (100) facets and their vicinal range on the ECS are discontinuous.[54,85] We evaluated the $r_f(T)/z_0(T)$ for Au(100) at 1123 K and corrected it via Eq. (7) by taking repulsive step interactions into account.[53] Since the discontinuity at the (100) facet is small, the corrected ratio of 0.112 is very close to the measured one, 0.108. The step free energy for reconstructed (100) islands at 353 K was determined via the fluctuation technique as 59 meV/Å (Ref. 62) which was upscaled to 1123 K using a kink energy of 70 meV (Ref. 63) and a vibrational entropy of 0.017 meV/K.[86] The value for the surface free energy is then 91 meV/Å^2 or 1.46 J/m^2

which compares well with published values of 1.40–1.53 J/m^2 for polycrystalline Au.[1]

For Pb we have trustworthy step free energies and 3D ECS data at four different temperatures between 323 and 550 K based on STM and SEM imaging at temperature.[14,57] The average surface free energy of Pb(111) at about 320–400 K is 27.5 meV/Å^2 or 440 mJ/m^2. This value is low but still compatible with previously published experimental surface free energies of Pb, 560–610 mJ/m^2,[29,87] since those presumably represent undefined high-index orientations. The (111) surface is expected to have the lowest surface energy, and secondly, the current value is close to a recently calculated value of 26 meV/Å^2 or 416 mJ/m^2 for this surface,[88] based on local density functional theory including the effect of surface relaxation. In general, however, theoretical data for Pb(111) surface energies cover a large range from 270 to 600 mJ/m^2.[14,39]

At this point one may wish to come to a general assessment of the evaluation and data comparison presented in Table I. One point seems to be obvious: the surface free energies obtained for Au and Pb are in reasonable agreement with previous experimental and theoretical results while those for Cu and Si are either totally out of bounds or showing an unusual amount of scatter. Several reasons may be put forward to rationalize this observation. First, Au and Pb are one noble and one fairly inert metal, such that surface contamination may not play a role. Second, the facets could be well located in both cases, due to the sharp edge at the Au(100) facet, on the one hand, and STM imaging of Pb(111), on the other hand. Third, step free energies were in both cases obtained by STM techniques.

For Si we have a large number of investigations, some involving STM imaging, others low-energy electron microscopy, SEM, TEM and REM, all of them having different resolution and vacuum environments. This holds for the determination of step free energies and step stiffnesses or of $r_f(T)/z_0(T)$ from the ECS of crystallites or voids. Different crystal sizes have been studied, a fact which may be responsible for some variation of the results. Note, however, that the absolute step free energies of vicinal Si(111)-1×1 are still uncertain. The theoretical $f_1(T)$ of Akutsu *et al.* for Si(111) was fit to data of Ref. 60 that had been obtained by assuming a surface free energy of 1.0 J/m^2. Hence our preferred data base, $f_1(T)$, for that surface is uncertain. The variability in results for Si(111) and (100) is then to be expected. Despite this caveat we note that averages of 0.76 and 1.13 J/m^2 are found for Si(111) and Si(100), respectively, with the anisotropy (100)/(111) being clearly larger than 1 when averaged over the measured range of temperature.

For Cu there is only a single investigation, in which the crystallites were equilibrated at high temperature, quenched to room temperature and then transferred to another system for SEM imaging.[24,64] The resulting surface free energies in Table I are too large and inconsistent with the known experimental and theoretical values of this quantity.[1,9,12,13] There are basically two possible explanations: either $f_1(T)$ of Cu is too large or $r_f(T)/z_0(T)$ is too small. Regarding the latter option, there are several possible shortcomings, such as unknown surface contamination, the quenching rate being too slow, or the facet radius being too small due to the low resolution of SEM. If the quenching rate were too slow, facets could have grown during quenching causing a larger $r_f(T)/z_0(T)$ ratio. However, this effect can be ruled out because it would mean even smaller $r_f(T)/z_0(T)$ ratios at the quench temperature. The influence of the other two factors on $r_f(T)/z_0(T)$ is difficult to assess. Cleanliness control by Auger electron spectroscopy and careful shape fitting of the facet-to-vicinal transition make it rather unlikely that these experimental factors are responsible for the unreasonably high values of the surface free energies of Cu in Table I compared to those obtained by theory and older experiments.[1]

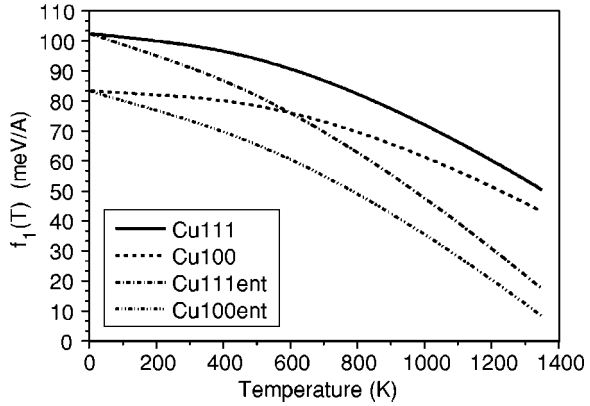

FIG. 5. Plot of temperature-dependent step free energies for vicinal Cu(111) and Cu(100) surfaces, all steps along close-packed ⟨110⟩ directions. The set labeled "ent" represents the higher vibrational entropies. See the text for further details.

The second possible shortcoming may be sought in $f_1(T)$ being too large. By treating the temperature dependence of the step free energy, we use a simple expression to extrapolate the step energies up to 1240 K from the low temperatures where they were actually measured. There are two parameters which govern the temperature dependence of the step free energy, the kink energy and the vibrational entropy.[2,89–92] One generally assumes the kink energy to be temperature independent, although this has not been proven. The vibrational entropy, on the other hand, may well be temperature dependent due to anharmonicity at high temperature. It is currently not possible to account for this in a physically accurate fashion[93] but by way of a rough approximation we include anharmonicity by choosing a larger average vibrational entropy contribution, compared to the harmonic values of 0.0325 meV/K for Cu(111) (Ref. 43) and 0.0173 meV/K for Cu(100) vicinal steps at low temperature. Consequently the step free energies at 1240 K will decrease. Figure 5 shows a comparison of the temperature dependence of $f_1(T)$ for Cu(111) and Cu(100) vicinal steps, calculated by using the vibrational entropies mentioned above and alternatively higher entropies of 0.095 and 0.083 meV/K for (111) and (100) steps, respectively. For the latter the step free energies at 1240 K are found at about 27 and 17 meV/Å, and the corresponding surface free energies are 119 meV/Å^2 for Cu(111) and Cu(100), respectively (or 1.9 J/m^2). The surface free energy anisotropy is negligible at this temperature.

Of course, the chosen values for the average vibrational entropies are arbitrary but not unreasonable in view of the large temperature gap between 320 K, where the step free energies were measured, and 1240 K where the ECS was formed and imaged after quenching. Future work will have to show whether this rationale can be substantiated.

IV. CONCLUSIONS

Absolute experimental step free energies and the geometry of a corresponding ECS, both at the same temperature T, can be used successfully to determine the surface free energy of a well-defined low-index orientation at T.

Utilizing the above approach, trustworthy surface free energies of Pb(111) and Au(100) are calculated which are consistent with previously published experimental and theoretical data.

Average surface free energies of 0.8 and 1.1 J/m^2 at 973–1373 K are obtained for Si(111)-1×1 and Si(100)-2×1, respectively. These values are below experimental and theoretical data known so far for Si.

Surface free energies of 4.0–5.5 J/m^2 are calculated for Cu(111) and Cu(100) which are far too high compared to the known experimental and theoretical values. Assuming a higher vibrational entropy to compute the step free energies at T (1240 K) improves the agreement with previously published data. The higher vibrational entropy may be justified by an increasing importance of anharmonicity at high temperatures.

ACKNOWLEDGMENTS

We gratefully acknowledge correspondence on the issue of Si step free energies with Ellen Williams, Jean-Jacques Métois, and Harold Zandvliet. We thank Dominique Chatain, Veronique Ghetta, and Paul Wynblatt for sending us the Cu ECS data and for continued discussion. H.P.B is grateful to Gerhard Ertl for supporting his stay at the Fritz-Haber-Institute (Berlin) where this paper was finished. M.N. would like to acknowledge the support of the University of Wroclaw under Grant No. 2016/W/IFD/05.

*Electronic address: h.bonzel@fz-juelich.de

[1] D. Sander and H. Ibach, in *Physics of Covered Solid Surfaces*, edited by H. P. Bonzel, Landolt-Börnstein, New Series (Springer, Berlin, 2002), Vol. III-42-A2, pp. 4.4-1–4.4-49.
[2] H. P. Bonzel and A. Emundts, Phys. Rev. Lett. **84**, 5804 (2000).
[3] H. P. Bonzel, Prog. Surf. Sci. **67**, 45 (2001).
[4] G. J. Ackland, G. Tichy, V. Vitek, and M. W. Finnis, Philos. Mag. A **56**, 735 (1987).
[5] P. Gumbsch and M. S. Daw, Phys. Rev. B **44**, 3934 (1991).
[6] M. Methfessel, D. Hennig, and M. Scheffler, Phys. Rev. B **46**, 4816 (1992).
[7] M. Mansfield and R. J. Needs, Phys. Rev. B **43**, 8829 (1991).
[8] H. S. Lim, C. K. Ong, and F. Ercolessi, Surf. Sci. **269–270**, 1109 (1992).
[9] L. Vitos, A. V. Ruban, H. L. Skriver, and J. Kollár, Surf. Sci. **411**, 186 (1998).
[10] P. J. Feibelman, Phys. Rev. B **62**, 17 020 (2000).
[11] I. Galanakis, G. Bihlmayer, V. Bellini, N. Papanikolaou, R. Zeller, S. Blügel, and P. H. Dederichs, Europhys. Lett. **58**, 751 (2002).
[12] I. Galanakis, N. Papanikolaou, and P. H. Dederichs, Surf. Sci. **511**, 1 (2002).
[13] F. Raouafi, C. Barreteau, M. C. Desjonquères, and D. Spanjaard, Surf. Sci. **505**, 183 (2002).
[14] C. Bombis, A. Emundts, M. Nowicki, and H. P. Bonzel, Surf. Sci. **511**, 83 (2002).
[15] G. Wulff, Z. Kristallogr. **34**, 449 (1901).
[16] C. Herring, Phys. Rev. **82**, 87 (1951).
[17] L. D. Landau and E. M. Lifshitz, *Statistical Physics* (Addison-Wesley, Reading, MA, 1958), Vol. V, p. 460.
[18] C. Jayaprakash and W. F. Saam, Phys. Rev. B **30**, 3916 (1984).
[19] M. Wortis, *Chemistry and Physics of Solid Surfaces*, edited by R. Vanselow and R. Howe (Springer-Verlag, New York, 1988), Vol. 7, p. 367.
[20] J. J. Métois and J. C. Heyraud, Surf. Sci. **446**, L127 (2000).
[21] W. W. Mullins and G. S. Rohrer, J. Am. Ceram. Soc. **83**, 214 (2000).
[22] G. S. Rohrer, C. L. Rohrer, and W. W. Mullins, J. Am. Ceram. Soc. **84**, 2099 (2001).
[23] M. Nowicki, A. Emundts, and H. P. Bonzel, Prog. Surf. Sci. **74**, 123 (2003).
[24] D. Chatain, V. Ghetta, and P. Wynblatt, Interface Sci. **12**, 7 (2004).
[25] M. Nowicki, C. Bombis, A. Emundts, H. P. Bonzel, and P. Wynblatt, New J. Phys. **4**, 60 (2002).
[26] D. Chatain and J. J. Métois, Surf. Sci. **291**, 1 (1993).
[27] E. D. Hondros, Proc. R. Soc. London, Ser. A **286**, 479 (1965).
[28] E. D. Hondros, in *Surface Energy Measurements*, edited by R. A. Rapp, Physicochemical Measurements in Metals Research, Techniques of Metals Research (Interscience, New York, 1970), Vol. IV, Part 2, p. 293.
[29] V. K. Kumikov and K. B. Khokonov, J. Appl. Phys. **54**, 1346 (1983).
[30] N. C. Bartelt, R. M. Tromp, and E. D. Williams, Phys. Rev. Lett. **73**, 1656 (1994).
[31] E. D. Williams and N. C. Bartelt, Science **251**, 393 (1991).
[32] H.-C. Jeong and E. D. Williams, Surf. Sci. Rep. **34**, 171 (1999).
[33] H. J. W. Zandvliet, Rev. Mod. Phys. **72**, 593 (2000).
[34] M. Giesen, C. Steimer, and H. Ibach, Surf. Sci. **471**, 80 (2001).
[35] M. Giesen, Prog. Surf. Sci. **68**, 1 (2001).
[36] A. Emundts, M. Nowicki, and H. P. Bonzel, Surf. Sci. **496**, L35 (2002).
[37] M. Nowicki, C. Bombis, A. Emundts, and H. P. Bonzel, Phys. Rev. B **67**, 075405 (2003).
[38] J. J. Métois and P. Müller, Surf. Sci. **548**, 13 (2004).
[39] H. P. Bonzel, Phys. Rep. **385**, 1 (2003).
[40] B. S. Swartzentruber, Y. W. Mo, R. Kariotis, M. G. Lagally, and M. B. Webb, Phys. Rev. Lett. **65**, 1913 (1990).

[41] H. J. W. Zandvliet, H. B. Elswijk, E. J. van Loenen, and D. Dijkkamp, Phys. Rev. B **45**, 5965 (1992).
[42] D. C. Schlösser, L. K. Verheij, G. Rosenfeld, and G. Comsa, Phys. Rev. Lett. **82**, 3843 (1999).
[43] C. Steimer, M. Giesen, L. Verheij, and H. Ibach, Phys. Rev. B **64**, 085416 (2001).
[44] G. Schulze Icking-Konert, M. Giesen, and H. Ibach, Phys. Rev. Lett. **83**, 3880 (1999).
[45] R. Van Moere, H. J. W. Zandvliet, and B. Poelsema, Phys. Rev. B **67**, 193407 (2003).
[46] A. Emundts, "Morphologie und Energetik kleiner Bleikristalle," doctoral thesis, RWTH Aachen, Germany, 2001.
[47] N. Akutsu and Y. Akutsu, J. Phys.: Condens. Matter **11**, 6635 (1999).
[48] M. Giesen-Seibert, F. Schmitz, R. Jentjens, and H. Ibach, Surf. Sci. **329**, 47 (1995).
[49] N. C. Bartelt and R. M. Tromp, Phys. Rev. B **54**, 11 731 (1996).
[50] R. C. Nelson, T. L. Einstein, S. V. Khare, and P. J. Rous, Surf. Sci. **295**, 462 (1993).
[51] D. Yu and M. Scheffler, to be published (2004).
[52] W. W. Mullins, Interface Sci. **9**, 9 (2001).
[53] A. Emundts, H. P. Bonzel, P. Wynblatt, K. Thürmer, J. Reutt-Robey, and E. D. Williams, Surf. Sci. **481**, 13 (2001).
[54] Z. Wang and P. Wynblatt, Surf. Sci. **398**, 259 (1998).
[55] K. Arenhold, S. Surnev, H. P. Bonzel, and P. Wynblatt, Surf. Sci. **424**, 271 (1999).
[56] J. C. Heyraud and J. J. Métois, J. Cryst. Growth **82**, 269 (1987).
[57] J. C. Heyraud and J. J. Métois, Surf. Sci. **128**, 334 (1983).
[58] A. Pavlovska, D. Dobrev, and E. Bauer, Surf. Sci. **326**, 101 (1995).
[59] C. Rottman, M. Wortis, J. C. Heyraud, and J. J. Métois, Phys. Rev. Lett. **52**, 1009 (1984).
[60] J. M. Bermond, J. J. Métois, X. Egéa, and F. Floret, Surf. Sci. **330**, 48 (1995).
[61] J. M. Bermond, J. J. Métois, J. C. Heyraud, and F. Floret, Surf. Sci. **416**, 430 (1998).
[62] C. Bombis and H. Ibach (unpublished).
[63] P. Stoltze, J. Phys.: Condens. Matter **6**, 9495 (1994).
[64] D. Chatain, V. Ghetta, and P. Wynblatt (unpublished).
[65] D. J. Eaglesham, A. E. White, L. C. Feldman, N. Moriya, and D. C. Jacobson, Phys. Rev. Lett. **70**, 1643 (1993).
[66] H. J. W. Zandvliet, S. van Dijken, and B. Poelsema, Phys. Rev. B **53**, 15 429 (1996).
[67] T. Suzuki, H. Minoda, Y. Tanishiro, and K. Yagi, Surf. Rev. Lett. **6**, 985 (1999).
[68] J. H. Wilson, J. D. Todd, and A. P. Sutton, J. Phys.: Condens. Matter **2**, 10259 (1990).
[69] D. M. Follstaedt, Appl. Phys. Lett. **62**, 1116 (1993).
[70] T. Suzuki, J. J. Métois, and K. Yagi, Surf. Sci. **339**, 105 (1995).
[71] J. Tersoff and E. Pehlke, Phys. Rev. B **47**, 4072 (1993).
[72] E. D. Williams, R. J. Phaneuf, J. Wei, N. C. Bartelt, and T. L. Einstein, Surf. Sci. **294**, 219 (1993).
[73] E. D. Williams, R. J. Phaneuf, J. Wei, N. C. Bartelt, and T. L. Einstein, Surf. Sci. **310**, 451 (1994).
[74] C. Alfonso, J. M. Bermond, J. C. Heyraud, and J. J. Métois, Surf. Sci. **262**, 371 (1992).
[75] K. Thürmer, D. J. Liu, E. D. Williams, and J. D. Weeks, Phys. Rev. Lett. **83**, 5531 (1999).
[76] S. D. Cohen, R. D. Schroll, T. L. Einstein, J. J. Métois, H. Aebremarian, H. L. Richards, and E. D. Williams, Phys. Rev. B **66**, 115310 (2002).
[77] A. Laracuente and L. J. Whitman, Surf. Sci. **476**, L247 (2001).
[78] R. J. Jaccodine, J. Electrochem. Soc. **110**, 524 (1963).
[79] R. D. Meade and D. Vanderbilt, Phys. Rev. B **40**, 3905 (1989).
[80] K. D. Brommer, M. Needels, B. E. Larson, and J. D. Joannopoulos, Phys. Rev. Lett. **68**, 1355 (1992).
[81] G. H. Gilmer and A. F. Bakker, Mater. Res. Soc. Symp. Proc. **209**, 135 (1991).
[82] I. Stich, M. C. Payne, R. D. King-Smith, J. S. Lin, and L. J. Clarke, Phys. Rev. Lett. **68**, 1351 (1992).
[83] M. Needels, Phys. Rev. Lett. **71**, 3612 (1993).
[84] P. J. Feibelman, Phys. Rev. B **60**, 11 118 (1999).
[85] J. C. Heyraud and J. J. Métois, Acta Metall. **28**, 1789 (1980).
[86] S. V. Khare and T. L. Einstein, Surf. Sci. **314**, L857 (1994).
[87] W. R. Tyson and W. A. Miller, Can. Metall. Q. **14**, 307 (1975).
[88] D. Yu and M. Scheffler, Phys. Rev. B **70**, 155417 (2004).
[89] A. Kara, S. Durukanoglu, and T. S. Rahman, Phys. Rev. B **53**, 15 489 (1996).
[90] A. Kara, S. Durukanoglu, and T. S. Rahman, J. Chem. Phys. **106**, 2031 (1997).
[91] J. W. M. Frenken and P. Stoltze, Phys. Rev. Lett. **82**, 3500 (1999).
[92] H. J. W. Zandvliet, O. Gurlu, and B. Poelsema, Phys. Rev. B **64**, 073402 (2001).
[93] T. S. Rahman, A. Kara, and S. Durukanoglu, J. Phys.: Condens. Matter **15**, S3197 (2003).